Dynamics of Isoelectric Precipitation of Casein Using Sulfuric Acid

G. W. Hofland, M. R. Berkhoff, and G. J. Witkamp
Laboratory for Process Equipment, Delft University of Technology, Delft, The Netherlands

L. A. M. van der Wielen
Kluyver Laboratory for Biotechnology, Delft University of Technology, Delft, The Netherlands

The acid precipitation of casein from skim milk is an interesting and complex operation, as it involves several mechanistic steps occurring simultaneously. Research has focused so far on the influence of static variables such as temperature and final pH on the curd properties. Here the dynamics of the process was investigated. From a characteristic times analysis it was concluded that the most important mechanistic steps in the acid precipitation of casein were acid mixing, aggregation/breakup, and transport in/out of the precipitate particles. Experiments in a fed batch setup using sulfuric acid as the precipitant showed how the precipitation influenced the pH profile and demonstrated the large influence of process variables, such as the acid addition rate, the mixing intensity, and aging time on particle-size distributions and the release of minerals from the casein.

Introduction

Food processing operations are often poorly understood processes. The common empirical approach of describing these processes conceals the complexity of the processes, not only for the chemistry but also for the transport of mass, heat, and impulse. The acid precipitation of casein from skim milk is such a process. The manufacture of acid casein involves isoelectric precipitation, whey separation, multistage washing, dewatering, and drying of the precipitate (Southward and Walker, 1980). The importance of the precipitation step for the final product yield and quality has been stressed by Jablonka and Munro (1985). The precipitation step determines the initial particle size, which is important for the efficacy of the solid–liquid separation, and the intent of undesired components such as calcium phosphate, which have to be washed out and which are important product quality parameters.

Nowadays the isoelectric precipitation uses mostly mineral acids. Two operating procedures are known (Cariç, 1994). In the first, the milk is heated to the precipitation temperature (40–55°C) and mixed with the acid solution. The resulting precipitate slurry is subsequently aged (acidulated). In the alternative process, the milk is first mixed with the acid at low temperatures. Then steam is injected into the mixture to increase temperature and induce precipitation. Here an aging step can be applied as well. The first process type is more generally applied, also for isolation of other proteins, and is, therefore, addressed in this article.

Several articles have been written on the influence of temperature and pH on the characteristics of the precipitate curd. Southward and Walker (1980) presented a graph in which the different types of casein curd, from soft and mushy to hard and brittle or rubbery, are categorized toward final pH and temperature. Jablonka and Munro (1986, 1987, 1988) present a series of articles on the influence of these variables on the particle size, particle strength (firmness and cohesiveness), and residual calcium. Different scales and modes of operation (batch/continuous) were investigated. An important result from this work was the correlation between the calcium levels and the other particle characteristics such as size and strength. Jablonka, however, only discussed the influence of the final conditions on the particle characteristics. The dynamics of the process, or in other words, the way the final conditions are reached, was not addressed, even though variations in acid mixing conditions were named as a possible

Correspondence concerning this article should be addressed to G. W. Hofland at this current address: Laboratory for Process Equipment, Delft University of Technology, Leeghwaterstraat 44, 2628 CA Delft, The Netherlands.

cause of differences in the results observed for the setups under investigation (Jablonka et al., 1986).

An investigation of the influence of mixing conditions on the coagulation rate was performed by Bhaskar et al. (1993). They related the particle formation with Schmoluchowski's theory of orthokinetic aggregation and found that the coagulation rate increased linearly with $Re^{3/2}$. In their work, a special setup was used that was intended to minimize breakup of particles, despite the high Reynolds numbers ($> 4 \cdot 10^4$). No link was made to influences of other process variables and the influence of mixing on mechanistic steps other than the coagulation.

In this work, the dynamics of the batch precipitation of casein using mineral acid was investigated. The mechanics of the process were investigated using a characteristic time analysis, as an onset to future modeling. Further, the influence of acid addition rate, stirring conditions, as well as aging time were quantified experimentally on the basis of on-line pH measurements and analysis of the size and water content of the particles and calcium and phosphate release to the whey.

Physical Model of Casein Precipitation

The precipitation of casein is a complex process, as it involves several process steps that occur in part simultaneously. Upon acidification (Walstra, 1990):

- Calcium phosphate clusters connecting serine phosphate groups of the proteins dissolve;
- Casein micelles swell;
- κ-Casein peptide chains, that initially protrude from the micelle surface into the solution, forming a "brush," collapse on the micelle surface, which strongly diminishes the resistance to coagulation;
- The micelle structure may fall apart, depending on temperature;
- Coions of negatively charged groups of the protein (viz., Ca^{2+} and Mg^{2+}) are exchanged for protons;
- Casein aggregates due to a decrease of both the electric charge and the steric hindrance;
- Water may be repelled from the protein precipitate leading to shrinkage.

Apart from the processes that occur in the protein (micelles), one can distinguish process steps, such as the transport of the acid to the protein. Accordingly, Jablonka et al. (1998) describe the precipitation process of casein as a five-step mechanism:

(1) Mixing of the acid with the milk;
(2) Diffusion of the protons into the micelle;
(3) Diffusion of dissolved calcium phosphate out of the micelle/precipitate;
(4) Precipitation;
(5) Aggregation and break-up of particles.

These mechanistic steps are discussed further below and, to investigate the importance of the different steps of the process, characteristic times were estimated.

Mass transport

The mixing of the precipitant solution with the protein solution is accomplished by a number of mechanisms that are active at different scales in the precipitator (macromixing, mesomixing, and micromixing). Apart from different length scales, these mixing mechanisms have different time scales (Table 1). The transport in casein micelles and precipitates is complex for a number of reasons. First, the transport involves diffusion of several components (Figure 1). The diffusion of the various ions, H^+, Ca^{2+}, phosphates, Mg^{2+}, citrates, among them, is electrostatically coupled and requires a Maxwell-Stefan modeling approach. Further, besides diffusion the transport involves drift as a consequence of swelling and shrinkage of the protein matrix. Casein micelles first exhibit swelling upon acidification. During the precipitation, the water content of the casein will decrease. According to Teo et al. (1996a), the water holding capacity of washed casein precipitate displays a minimum around 5.0–5.3. The driving force for the flux of water may hence change direction during the process. Along with other authors (O'Meara and Munro, 1982), Teo et al. (1996b) also observed shrinkage when the curd was washed, an effect of changing ionic strength. Finally, the swelling and shrinkage of the protein causes drift and causes the diffusion coefficients in the precipitate gel to change in the course of time, depending on the pH and ionic strength. Diffusion in gels can be related to the volume fraction of the protein matrix (ϕ) by using Ogston's equation (Vonk, 1994)

$$D_p = D_0 \cdot e^{-(1+\lambda)\cdot\sqrt{\phi}} \tag{1}$$

In Eq. 1, λ equals r_s/r_p, where r_s is the size of the diffusing solute and r_p is the size of the matrix fiber.

Table 1. Time Constants for Mass Transport

Macromixing	$t_{\text{circ}} = \dfrac{V}{r_c N_q d_s^3 N}$	(2)
Micromixing	$t_{mm} = 0.1 \cdot \dfrac{\lambda_k^2}{D} = 0.1 \cdot \dfrac{\nu^{3/2}}{\epsilon^{1/2} D}$	(3)
Transport in particles	$t_d = 0.1 \cdot \dfrac{d_p^2}{D_p}$	(4)

Source: Thoenes (1994).

Precipitation

The precipitation mechanism of proteins such as casein is fully dominated by aggregation (Bell, 1983). Since no crys-

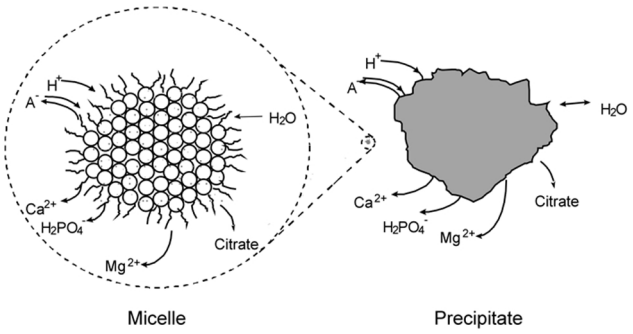

Figure 1. Diffusion of ions upon acidification in casein micelles and precipitates; " A" denotes the acid coion.

talline phase is formed, nucleation and growth can hardly be recognized as individual steps in the mechanism. Four mechanisms for the collision of particles can be distinguished: diffusion, shear, inertia, and gravity. The mechanism that is predominant depends on the size of the particles. The rate of the aggregation mechanisms is usually second order in the particle concentration (Söhnel and Garside, 1992).

In casein precipitation, particle sizes can be as high as 5 mm, and, therefore, all of the collision mechanisms previously referred to will take place, although the effect of Brownian motion on the particle size can be ignored. For inertia and gravitation-induced aggregation, no characteristic time can be defined without input of a particle-size distribution. The characteristic time for shear-induced precipitation is (Söhnel and Garside, 1992)

$$t_p = \frac{\pi}{4\alpha\phi_{\text{vol}}G} \tag{5}$$

where G is the shear rate, α is a factor indicating the probability of a successful collision, and ϕ_{vol} is the volume fraction of particles. Here G is calculated from (Camp and Stein, 1943)

$$G = \sqrt{\frac{\epsilon}{\nu}} \tag{6}$$

The energy dissipation (ϵ) is often replaced by an average value. The validity of such averaging is doubtful, because the local energy dissipation near the stirrer is usually much higher—up to 50 times—than in the bulk. In the acid precipitation of casein, where particle sizes exceed the Kolmogorov length scale and the particle concentrations are high, the situation is even more intricate because the precipitation will influence the flow pattern and vice versa. Compartment models, suggested for incorporating effects of concentrations or shear variations in crystallization processes (Van Leeuwen et al., 1996), are not easily applied here, because of the changes in the hydrodynamic regime. Locally, the viscosity may increase greatly and gel formation may occur. Many aggregation kernels theoretically predict gellation for high aggregation rates (Smit et al., 1994), but are not applicable in highly concentrated suspensions.

Casein precipitation kinetics have been investigated by Kinsella and coworkers (Bringe and Kinsella, 1990, 1991; Kim and Kinsella, 1989). They strongly reduced the protein concentration (diluted up to a 1,000-fold) to be able to investigate the fast precipitation process. These investigations aimed at quantifying the effects of pH and temperature on the precipitation rate as well as the influence of inorganic additives, such as calcium and several anions. Although the strong dilution used in the investigations makes it impossible to resolve absolute values for aggregation rates in undiluted skim milk, the results are useful for determining the relative effect of temperature and pH on the collision efficiency.

The aggregation rate as a function of pH exhibited a parabolic curve, starting off at pH 5.1 and having a maximum around pH 4.6 (Bringe and Kinsella, 1990). The pH is therefore an important factor on the rate at which the precipitation proceeds. Temperature was also found to strongly affect the aggregation rate. Kim and Kinsella (1989) found the maximum rate to rise a factor of 2 and 2.4 at 45°C and 55°C relative to 35°C.

Breakup

As soon as particles are formed, they are also subject to breakup. Breakup of protein particles is considered to be induced by the local hydrodynamic field rather than by particle collisions. The particle breakup is therefore first order in the particle concentration (Bell et al., 1983). Generally, the precipitate breakup rate strongly increases with increasing particle size and increasing (local) energy dissipation (Vanni, 2000). A characteristic time for breakup rate is however hard to estimate, because the particle strength depends—apart from the properties of the precipitated compound—on the course of conditions during the precipitation (Brown and Glatz, 1987). The breakup process also influences the transport of solutes out of the precipitates. Breakup diminishes the length over which diffusion takes place and its stochastic character is an extra complication in modeling the transport of solutes from the precipitate particles.

Characteristic times

Characteristic times were estimated for two values of the power input. The input values of the characteristic time analysis were chosen such that the calculated numbers were relevant for the lab-scale experiments performed in this study (Table 2). The specific power input was calculated from the following equation

$$\epsilon = 4N_p N_s^3 d_s^5 / \left(\pi d_t^2 h_t\right) \tag{7}$$

where N_p is the power number, N_S is the stirring rate, and d_S is the diameter of the stirrer. The power number, which varies with Re, was taken from Janssen and Warmoeskerken (1987).

As an indication of the rate of the diffusion process in micelles and precipitate particles, the characteristic times of the largest (hydrated) ion (calcium) were calculated. The radius of the hydrated calcium ion is 0.36 nm. For casein micelles,

Table 2. Values of the Parameters as Used in the Characteristic Time Analysis

V	0.9	L	D	In solution	8.3×10^{-10}	m^2/s	(hydrated Ca; 40°C)
d_t	103	mm		In micelles	2.7×10^{-10}	m^2/s	
h_t	103	mm		In precipitate	1.8×10^{-10}	m^2/s	
d_s	36	mm	η		1×10^{-3}	$kg\cdot(m\cdot s)^{-1}$	(40°C)
N_p	1	—	ρ_l		1,026	$kg\cdot m^{-3}$	(40°C)
N_q	0.8	—	d_{micelle}		200	nm	
r_c	1.5		$d_{\text{precipitate}}$		1	mm	

the solids content is ~22% (De Kruijf, 1998). For precipitate particles, the solid content is typically 50% (Pearce et al., 1987). The size of the matrix was estimated to be 0.5 nm (Stryer, 1988). The size of the casein micelles ranges from 20 nm to 200 nm. The largest size was used in the calculation.

The resulting characteristic times are recorded in Table 3 for two stirring rates. Two consecutive stages in the process can be recognized, that is, the aggregate formation and the aging. The aggregate formation stage is controlled by the liquid mixing and the precipitation. The aging stage, the diffusion in and out of the micelles competes with the breakup of the precipitate.

The calculations indicate that the diffusion limitation is negligible for casein micelles, even when a diffusion coefficient is assumed to be a 100 times smaller than in solution. The diffusion of ions in and out of the micelles can therefore be neglected when studying the influence of the dynamics of the total process on the product characteristics. One would expect the same is true for the other processes in the micelles, such as the swelling and the dissolution of calcium phosphate.

For precipitate particles of sizes of 1 mm, the diffusion limitation is considerable. This is important when considering the composition of the casein precipitate and determining the required aging period. Upon precipitation, the precipitate may contain calcium, as not all of the calcium has been liberated at the pH at which precipitation starts (Le Graët and Gaucheron, 1999).

It can be concluded that the precipitation process can be faster than the macromixing, which means that the precipitation is determined by local conditions. The extent to which concentration variations become relevant for the precipitation depends on the amount of acid supplied per unit time and its effect on the precipitation via the pH-dependent collision rate.

This characteristic time analysis shows what mechanical steps can be expected to be important. The following are still unknown, however:

- Effect of the pH in the precipitation at industrially relevant concentrations;
- Effect of mixing conditions on particle formation;
- Effect of conditions during particle formation on the breakup process;
- Effect of the precipitation conditions on the release of minerals from the precipitate.

Modeling Calculations

The preceding analysis indicated the limitations of the knowledge of the process. Modeling was restricted to a calculation of the pH profiles during the acidification and aging stages. For this calculation of the pH profiles, the acid addition and the diffusion from the precipitates were taken into account. The calculation is further confined to cases where particle breakup could be neglected. The pH from a solution of varying composition can be calculated using the electroneutrality condition

$$\sum_i \nu_i \cdot m_i = 0 \tag{8}$$

where ν is the valence and m the molality of the specific ion. The milk–salt system is difficult to describe due to the large number of—often weak—electrolytes and complexes (Holt et al., 1981; Van Dijk, 1990). This can be overcome by making use of the titration curves of skim milk and whey, from which the uptake of the protons by the constituents of the mixture can be determined. The titration curves for reconstituted skim milk made from the same batch of milk powder as used in this study are presented in Hofland et al. (1999). The number of protons associating with the skim milk constituents (casein, whey proteins, salts, and so on) was determined by substracting the number of free protons in solution from the number of protons added during the titration. For the situation where sulfuric acid is added to skim milk, Eq. 8 then reduces to

$$m_{\mathrm{H}^+} - \frac{K_w}{m_{\mathrm{H}^+}} - 2 \cdot m_{\mathrm{SO_4}^{2-}} + uptake_{milk}(pH) \cdot \mathrm{c}_{\mathrm{mp}} = 0, \tag{9}$$

where K_w is the dissociation constant of water, c_{mp} is the concentration of the milk powder (kg/kg), and $uptake_{milk}$ is the number of protons reacting to the milk constituents, which was described by

$$\mathrm{uptake(pH)} = A + B \cdot \mathrm{pH} + C \cdot e^{\mathrm{pH}} + D \cdot e^{-\mathrm{pH}} \tag{10}$$

The values of the coefficients are displayed in Table 4. The molality of the protons relates to the pH via

$$m_{\mathrm{H}^+} = 10^{-\mathrm{pH}}/\gamma \tag{11}$$

Table 3. Characteristic Numbers of the Precipitation of Casein

Stirring Rate		500	750	rpm
Reynolds number		11,100	16,640	—
Power number		0.85	0.76	—
Power input	Average	0.03	0.10	W/kg
Shear rate	Average	187	325	s^{-1}
Characteristic time	Liquid mixing: macro	1.9	1.25	s
	micro	0.05	0.03	s
	Precipitation: ($\alpha = 1$)	0.04	0.02	s
	($\alpha = 0.1$)	0.35	0.20	s
	($\alpha = 0.01$)	3.5	2.0	s
	Diffusion in/out micelles	2×10^{-5}	2×10^{-5}	s
	Diffusion in/out precipitates	545	545	s

Table 4. Values of Coefficients in Eq. 10

	A	*B*	*C*	*D*
Milk	2.67	−0.46	5.18×10^{-4}	−7.13
Whey	−2.98	1.03	1.99×10^{-4}	35.98

where γ is the activity coefficient of the proton, which was taken from the Debye–Hückel equation. The activity coefficient varies between 0.72 and 0.77 kg/mol, because the ionic strength during the process increases from 0.08 mol/kg to 0.14 mol/kg, a consequence of the dissolution of the calcium phosphate. The average, 0.75 kg/mol, was taken in the calculations.

For a given acid addition ($m_{SO_4^{2-}}$), the pH can be calculated from Eq. 9 for the situation where no precipitation has occurred. When precipitation occurs, the accessibility of protons is limited by diffusion in the precipitate phase. In a first, rough approximation, the diffusion can be modeled by applying Newton's cooling law for mass transfer (Bird et al., 1960)

$$\ln\left(\frac{m_1-\langle m\rangle}{m_1-m_0}\right)=\frac{Sh\cdot D}{d_p}\frac{A_p}{V_p}t \qquad (12)$$

where $\langle m\rangle$ is the average molality in the particle at a certain time, t; m_0 and m_1 are the initial concentration and the surface concentration; respectively; A_p and V_p are the particle surface and volume, respectively; and Sh is the Sherwood number (= 6.6 for a sphere).

The preceding equation cannot be used for the leveling of actual components between the particle and its surroundings, because the concentrations of the whey phase vary, as do the concentrations in the particles. To avoid elaborate modeling of the concentrations of all major components, two pseudocomponents were defined, one reflecting the uptake of protons by the casein precipitate and the other reflecting the proton uptake by the whey components. The uptake of protons by whey constituents was determined from a titration of whey after casein removal by ultracentrifugation (20,000 g; 2 h). Substracting the proton uptake by the whey from the proton uptake from the total skim milk gives the uptake by the casein precipitate. Equation 12 can be applied to the casein precipitate pseudocomponent when particle-size changes are neglected. The average fraction of the precipitate in equilibrium with the whey phase can then be approximated by

$$\left[1-e^{-Sh\cdot D\cdot 6/d_p^2\cdot(t-t_{coag})}\right].$$

Applying this factor in the electroneutrality condition (Eq. 9), gives

$$m_{H^+}-\frac{K_w}{m_{H^+}}-2\cdot m_{SO_4^{2-}}+\Big[\text{uptake}_{whey}(\text{pH})+\text{uptake}_{prec.}(\text{pH})\cdot\left[1-e^{-Sh\cdot D\cdot 6/d_p^2\cdot(t-t_{coag})}\right]\Big]\cdot c_{mp}=0 \qquad (13)$$

where t_{coag} is the time at which coagulation occurs. It is assumed that the particle size does not change during the process. That is, the aggregation process is fast in comparison with the diffusion process, and breakup or shrinkage of particles can be neglected. Equation 13 uses a lumped coefficient for the diffusion of the various components.

Materials and Methods

Equipment

The precipitation experiments were performed in a setup consisting of a glass-jacketed stirred vessel 104 mm in diameter. The stirring was a standard Rushton turbine impeller, 36 mm in diameter, which was placed at one-third of the liquid height. The acid was added via a tube (inner diameter 1 mm) placed at 1 cm from the stirrer and at 1 cm below the liquid level.

An epoxy-lined pH electrode (6 mm in diameter; Broadley-James, CA) was inserted at 2.5 cm from the wall and at 5 cm from the bottom, opposite to the acid inlet. No baffles were applied to prevent precipitate from piling up behind these obstacles. A dosage controller was used for the acid addition (Dosimat 665; Metrohm Herisau, Ch).

Experiments

Reconstituted milk was made by dissolving low-heat milk powder in demineralized water to give a 10 wt % solution. The concentration of casein was determined to be 2.7 wt %. The milk was stabilized by first keeping it at room temperature for half an hour and then keeping it at 40°C for another half an hour, before starting the experiment.

A series of experiments was carried out using a 0.5-M sulfuric acid solution to determine the influence of the rate of acidification, the aging period, stirring rate, temperature, and the amount of acid added. In each experiment a known quantity of sulfuric acid was added in a certain period, the acidification time, at a constant rate, which was followed by a certain aging period. The precipitation experiments were performed at 40–50°C, which is the normal temperature range applied in industry (Southward and Walker, 1980). The temperature was generally kept at 40°C, because at this temperature the particle sizes were still reasonably small in comparison with the size of the equipment. The volume of the acid solution was normally kept at 50 mL, which is 57 g per kg of reconstituted milk. This amount corresponds to an equilibrium pH of 4.63 for this batch of milk powder at 40°C (Hofland et al., 1999). The acidification time was varied between 1 and 16 min. Most experiments, however, were performed at 1, 4, and 6 min. In some experiments, the rate was changed during the experiment to determine the influence of exposure to different pH regimes. The aging period was defined to start directly after the acid solution was supplied. The aging time varied between 1 and 24 min, but 1 min and 10 min were taken as standards when other variables were varied. Stirring rates of 500 rpm and 750 rpm were tested. Table 3 shows the hydrodynamics characteristics at these rates.

During the experiments, the pH and temperature were monitored on-line. The response was tested by dipping the pH electrode into a stirred acidified milk solution. The electrode response was best fitted using a logistic dose-response equation

$$\text{pH}=\text{pH}_\infty+\frac{(\text{pH}_0-\text{pH}_\infty)}{1+(t/t_{er})^{\delta}} \qquad (14)$$

where the fitted values for t_{er} and δ were 2.67 s and 1.52. The characteristic time for the response delay can be taken to be equal to the parameter t_{er}. Its value is of the same order as the macromixing time. Transient effects in poorly mixed locations in the vessel can therefore not be expected to be measured correctly. During the experiments, the pH was measured while stirring, which may result in deviations due to the disturbance of the electric field around the electrode. However, the effect of stirring appeared to be small; in practice, pH measured in milk while stirring differed less than 0.05 from values measured at stagnant conditions. On some occasions, the pH electrode was clogged by precipitate and a good profile could not be determined.

Analyses

The particle size of the casein precipitate was determined by a wet-sieving technique developed by Jablonka et al. (1985). In this method the precipitate is hardened by iron alum before sieving in order to prevent caking onto the sieves. A saturated solution of ferric ammonium sulfate ($FeNH_4(SO_4)_2 \cdot 12H_2O$) was added to the precipitate slurry in equal volumes and gently mixed. After 15 min the mixture was wet-sieved over eight stainless-steel mesh screens using normal tap water for spraying. The minimum mesh size was 75 μm in each analysis. The other sizes were varied, depending upon the expected particle-size range. The fractions were dried overnight in an oven at 80°C and weighed. The impact of the sieving method on the particle was tested by mixing the sieved fractions of a typical sample and sieving them again. From the weight of the wet fractions, the particle size was 6% smaller in the second run relative to the first.

The method for measuring the solids contents of the casein precipitate was adopted from O'Meara and Munro (1982). The casein curd was separated from the whey using a stainless steel mesh screen (100μm) and drained during 5 min. The curd was evenly distributed over the screen. Comparing the mass of the drained curd and the dried curd gave the solids content. The drying procedure was the same as for drying the fractions.

The calcium and phosphate contents were determined from the supernatant solution using induced coupled plasma with atomic emission spectrophotometry detection (ICP-AES). First, the residual protein fraction was removed from the supernatant by precipitation with 24% trichloro acetic acid and subsequent centrifugation. After further dilution with a 2% HCl solution, calcium, phosphorus, sodium, and potassium concentrations were then analyzed in fivefold using scandium as an internal standard. A maximum variation of 5% was allowed in the analysis repeatability.

Results and Discussion

pH Profiles during batch precipitation

The dynamics of the precipitation process was investigated on the basis of measurement of the pH, the particle properties, and the release of minerals to the whey phase. The pH was the only variable measured on-line and used for monitoring the process. The pH-electrode was mounted opposite to the acid inlet and intended to measure the pH in a well-mixed region to avoid deviations due to imperfect mixing.

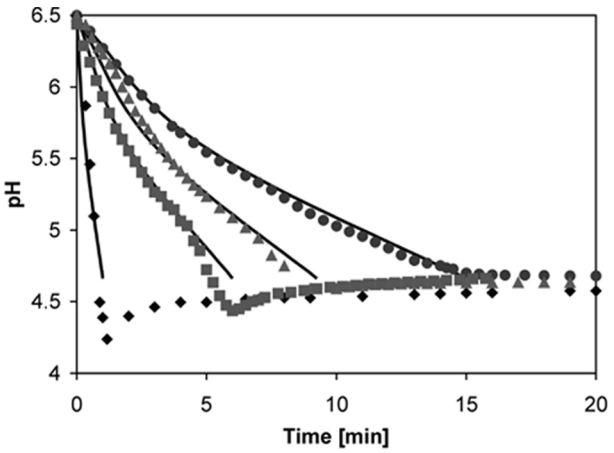

Figure 2. pH profiles during acidification at different acidification rates: ♦ 1 min; ■ 6 min; ▲9 min, and ● 16 min. Stirring rate 500 rpm, temperature 40°C. Lines represent values calculated by Eq. 9.

Figure 2 shows the pH profiles for a number of experiments. Not all the experiments gave such smooth pH profiles as shown here. At short acidification times (1 min), pH values scattered, particularly after precipitation, suggesting the imperfect mixing conditions. In some experiments, deviations occurred due to the clogging of precipitate around the pH electrode. Apart from that, the profiles were fairly well reproducible, as can be seen in Figure 3 for series at two acidification times.

The precipitate started to become visible after about 60% of the total amount of acid was added, at pH values around 5.1–5.0, as small particles that would rapidly grow. During the precipitation, the color of the continuous phase changed from opaque white to a clear pale yellow. The precipitation was accompanied by a sudden change in the rate of change of the pH, which is particularly well seen as a point of inflection in the curves for acidification times of 6 min and 9 min (Figure 2). It is believed that precipitation at this point causes the buffering groups of the protein and residual micellar calcium phosphate to become less accessible to the added acid. The fact that the point of inflection is located at a pH around 5.1–5.0—whereas the casein is known to precipitate at least

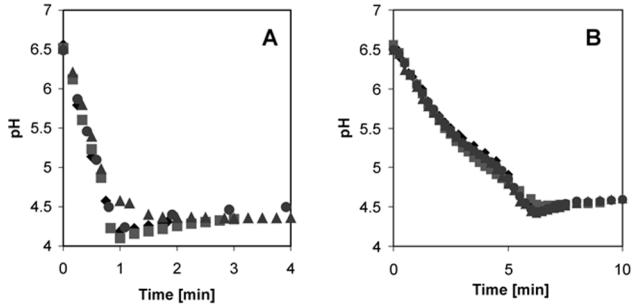

Figure 3. Variation of pH profiles in four experiments with acidification times of (A) 1 min and (B) 6 min.

partially at a higher pH—suggests that the characteristic time for precipitation at a pH above 5.1 is smaller than the acid addition time.

Besides the experimental values, Figure 2 also shows the model values, calculated from Eq. 9, which assumes no mixing and diffusion limitations. For most experiments, the experimental curves follow the calculated curves well in the range where the pH is larger than 5.1. For the experiment with the shortest acid addition time (1 min), the measured values were a little higher than calculated. At these high addition rates, however, the assumption that mixing limitations are absent is disputable. The expected deviations in pH by imperfect mixing can be estimated by relating the acidification time to the calculated macromixing time. During the acidification, the pH changes from 6.5 to 4.6. For an acidification time of 1 min, the pH changes on average 0.06 in a period equal to the calculated macromixing time (1.9 s). In addition to imperfect mixing, the response of the pH electrode may be a cause for the deviation. The response time of the electrode was of the same order as the calculated macromixing time (2.6 s vs. 1.9 s).

The experimental points start to deviate below pH 5.1, because the buffering groups of the precipitating casein that are not instantly accessible due to diffusion limitations. In Figure 4 the experiment with an acidification time of 6 min is highlighted. In this experiment, mixing can be regarded as fast in comparison with the acid addition; deviations in pH due to imperfect mixing are expected to be below 0.01. Figure 4 shows that the rate of change of pH suddenly shifts. The slope starts to follow the curve, taking only the uptake of protons by whey components into account, indicating that almost all casein must have precipitated and that the aggregation had proceeded to such an extent that diffusion in the precipitate became limiting. These measurements confirm the visual observation that the precipitation is rapid, relative to the acid addition.

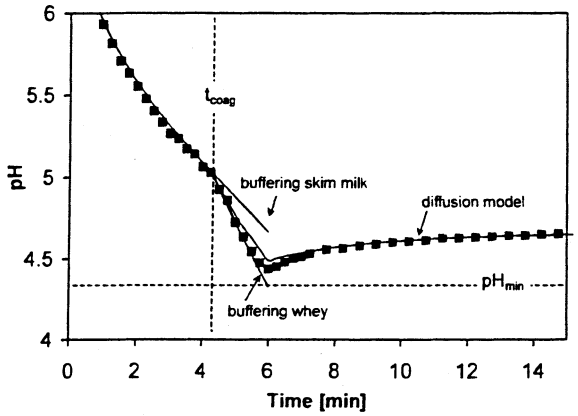

Figure 4. Change in slope in the pH profile upon precipitation.

Acidification time: 6 min. Lines: calculated values. Markers: experimental values (average of three experiments).

After the total acid addition, the pH rises to values close to the equilibrium value that indicates that most of the reactive groups were accessed within the time frame of the experiments. The diffusion process in the precipitate takes place within minutes, and is already effective during the last part of the acid addition (Figure 4). Without any diffusion in and out of the precipitate during the acidification period, the expected minimum in the pH curve would lie at pH 4.32. For an acidification time of 6 min, the experimental value lies at 4.43. At short acidification times, the minimum pH becomes even lower than the theoretical 4.32. For an acidification time of 1 min, values as low as 4.2 were recorded (Figure 2). This shows that the suspension could not be regarded as being well mixed at the position of the pH-electrode. When moving the pH electrode closer to the acid inlet, the nonideal mixing was even more apparent; pH values as low as 3.5 were mea-

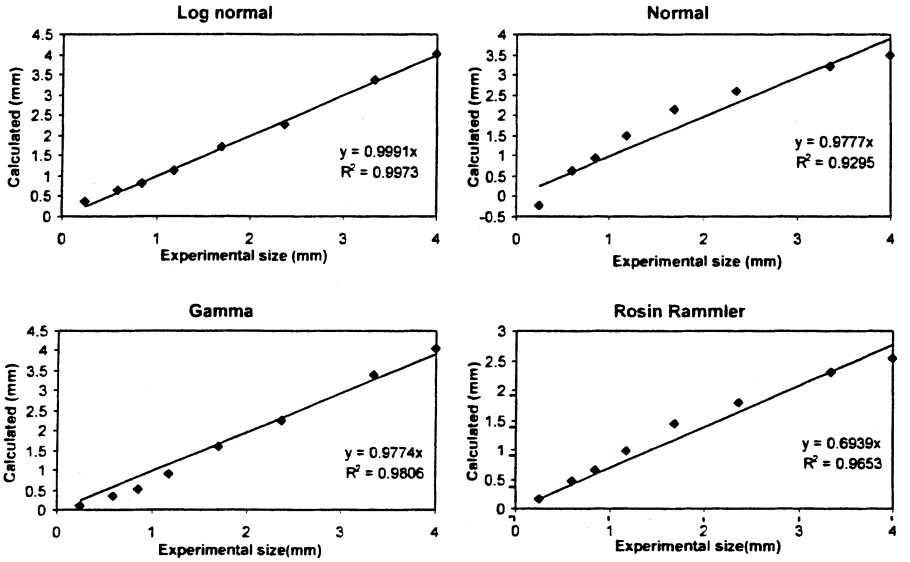

Figure 5. Parity plots of the fits of different cumulative particle size distributions for batch precipitation with 0.5 M sulfuric acid.

Conditions: pH 4.7, acidification time 3.5 min, 500 rpm, 40°C, aging 10 min.

sured. This will certainly affect the particle formation, and the modeling of the precipitation process should therefore account for spatial variation in the pH.

The diffusion was incorporated in the simulation of the pH-profile (Figure 4), using the model presented in Eq. 13. For the general case, predicting the pH profile is complex, particularly as a consequence of the possible shrinkage and breakup of the particles during aging. For acidification times of 6 min or longer, however, the particle size changed only little during aging (see Figure 10) and, therefore, the change in particle size was neglected. It was assumed that spherical particles 1.4 mm in diameter formed instantly at t_{coag}, where pH was 5.05. Also ignoring that we have a distribution of particle sizes, the diffusion coefficient for the process was fitted as $2 \cdot 10^{-10}$ m^2/s, using the least-square method.

Particle morphology and size

The particles formed in the process were dense aggregates. The size of the particles ranged between 0.1 and 5 mm. The particles were slightly elongated in shape, particularly those in the midsize fractions. Microscopic inspection did not reveal discernable primary particles. The larger particles could however be broken up into particles of 0.5–1.5 mm. Experimental particle-size distribution functions for particle formation processes can take one of several forms. Normal, log-normal, gamma, and Rosin-Rammler distributions have been used to describe distribution functions (Söhnel and Garside, 1992). For a typical experiment, parity plots are given for these particle-size distributions in Figure 5. It was found that in this work the data were best fitted with either the log-normal distribution or the gamma distribution. The good fit of the log-normal distribution is in accordance with Wilcox et al. (1979), who found that this distribution should be found for processes that involve random binary collisions between growth units. The normal distribution, which was found to be the best fitting by Jablonka and Munro (1986), was generally performing significantly less well for the whole range of experiments.

Influence of the acidification rate on the particle size

The influence of the acidification rate was measured in two series of experiments that differed in aging times (1 and 10 min). Particle-size distributions are shown in Figure 6. The mean particle sizes of the distributions are plotted as a function of the time during which the acid was added at a constant rate (Figure 7). Experiments performed in duplicate showed deviations of 0.5 mm at short acidification times (1 min) and 0.2 mm at longer acidification times (6 min).

The mean particle size decreased with increasing acidification time, both for short and long aging times. This is most pronounced in the series of the 1-min aging period. The mean particle size decreases from 3 mm at an acidification time of 1 min to around 0.5 mm at times of 10 min or larger. The large particles produced at high acidification rates are easily being broken up, which is indicated by the relatively large difference between the values at 1-min and 10 min for small acidification times. This phenomenon was also easily visible. At very small acidification times ($\leq$2 min), very large particles were formed that also strongly influenced the flow. Even

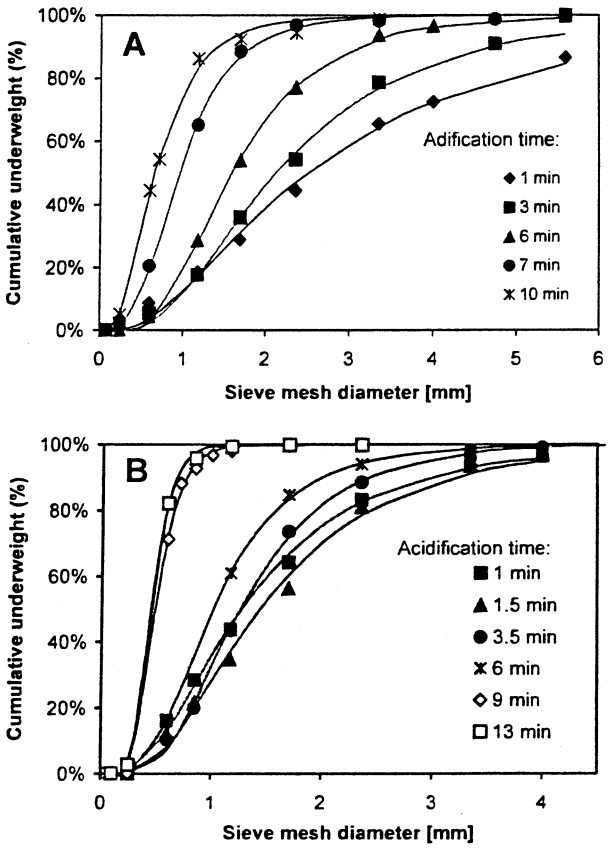

Figure 6. Cumulative underweight particle size distributions at different acidification times.

(A) Aging time 1 min; (B) aging time 10 min. Temperature 40°C; stirring rate 500 rpm. Markers: experimental; lines: fit log-normal distribution.

local stagnant spots in the vessel were observed during the acidification. In these cases, however, the flow resumed after a short aging time (about 5–20 s) due to the breakup of the connections between and within the particles.

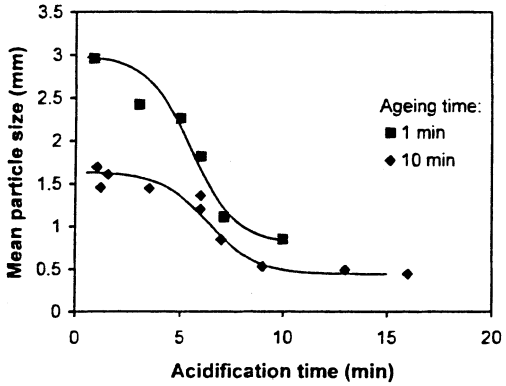

Figure 7. Experimental mean particle size in precipitation of casein with 0.5 M sulfuric acid applied at different feeding rates: temperature 40°C; stirring rate 500 rpm; lines to guide the eye.

The decrease in the particle size at longer acidification times can be explained in terms of characteristic times. Increasing the acidification time makes the characteristic time for mixing relatively short; absolute differences in the acid concentration due to imperfect mixing are smaller. The same reasoning would be expected for the characteristic precipitation time, if it was not a function of pH. A longer acidification period implies that more time is available for precipitation at high pH values, where the precipitation is a slow process. Also more time is allowed for breakup, leading overall to smaller particles. The higher degree of mixing can be attributed to this effect when the collision efficiency increased more than linearly with a decrease in pH.

Distinction of the influence of the acidification rate prior and during precipitation

Apart from the effects mentioned earlier, molecular processes preceding the precipitation could influence particle size. De Kruif (1998) mentions supra-aggregates of micelles before actual precipitation. Dalgleish and Law (1989) have shown that casein micelles disintegrate upon a decrease of pH. Despite the fact that the fraction of casein micelles that disintegrates was small at elevated temperatures—less than 10% at a temperature of 30°C—it could influence the precipitation. An increase in the dissolved protein concentration increases the viscosity. An increase in the viscosity diminishes the shear rate and consequently the aggregation rate. In addition, the building blocks of the precipitation may become smaller. The primary particle size was shown to influence the final aggregate size in soy protein precipitation (Nelson and Glatz, 1985).

To distinguish between those factors acting prior to and those acting during precipitation, a series of experiments was performed in which the acid addition rate changed after a 50% addition and after an 85% addition, corresponding to pH values of around 5.3 and 4.8, respectively. Table 5 shows that changing the acidification time for the first 50% of the acid between 2.5 to 7.5 min hardly influences the particle size, indicating that processes occurring prior to the precipitation did not affect the precipitation. Note that this assertion is of course only valid for processes that occur within the time frame of the experiments. The change in acidification time during the second half did influence the particle size, as expected.

Similar to the question whether the acidification rate before precipitation influenced the particle formation, one could ask whether the whole acidification period after the first precipitates emerged is of importance. Changing the acidification rate after adding 85% of the acid (~pH 4.7–4.8), influenced the particle size only to a small extent (Table 6). This could be expected, considering the fact that practically all the casein precipitates below a pH of 5.0 at 40°C, and so the driving force for precipitation does not change. Despite this, several authors mention the influence of pH on the precipitation in the pH range below 4.8 (Jablonka, 1986, 1987; Teo et al., 1996b). This experiment shows little effect, indicating that the progress of the aggregation and breakup processes have evolved to such an extent during the first stage of the precipitation that the rate of acid addition in the lower pH range does not attribute much to the increase in the particle size.

Table 5. Acidification Time Effect on Particle Size, When the Acidification Rate is Changed after Adding 50% Acid

Acidification time (min)		Aging time	Mean Particle
< 50%	> 50%	(min)	Size (mm)
2.5	2.5	1	2.26
3.3	2.5	1	2.24
5.0	2.5	1	2.52
7.5	2.5	1	2.46
5.0	1.3	1	3.29
5.0	2.5	1	2.52
5.0	5.0	1	0.85

Note: Temperature: 40°C; stirring rate 500 rpm.

Table 6. Acidification Time Effect on the Particle Size, When the Acidification Rate is Changed After Adding 85% Acid

Acidification time (min)		Aging time	Mean Particle
< 85%	> 85%	(min)	Size (mm)
5.1	0.45	1	1.84
5.1	0.9	1	1.82
5.1	1.5	1	1.69

Note: Temperature: 40°C; stirring rate 500 rpm.

Influence of the aging time on the particle size

The particle-size distributions are shown in Figure 8. Experiments in which the aging time was varied show that the large particles produced by fast acidification (1 min) are readily broken up (Figure 9 closed symbols). The experiments with long acidification times exhibit a smaller decrease in particle size. It must be noticed that breakup also will occur during the acidification stage. Aging time is not similar to the time allowed for breakup, particularly in experiments with longer acidification times. To take this into account, the experiments were also compared by plotting the particle size against the total time after coagulation occurred (Figure 9 open symbols). The curves for rapid acidification (1 min) and slow acidification (6 min) are now closer together, but the difference between the rapidly precipitated and the slowly precipitated particles remains significant. The mean particle size seems to become even smaller than that for the more slowly acidified casein (6 min), which would indicate that the fast precipitation leads to weaker particles, a phenomenon that is frequently observed in flocculation processes (Brown and Glatz, 1987). Also the fact that the pH was lower during aging in the case of rapid acidification (Figure 2) may have attributed to increased breakage. According to Teo et al. (1996a), the water uptake by precipitate curds increases at pH below 5.0–5.3 and, according to the results of Jablonka et al. (1986), the particle strength correlates with the solids content.

Influence of power input by stirring on the particle size

The power input plays a role in several parts of the precipitation dynamics. A higher power input decreases the mixing time and increases the aggregation rate (Bhaskar et al., 1993),

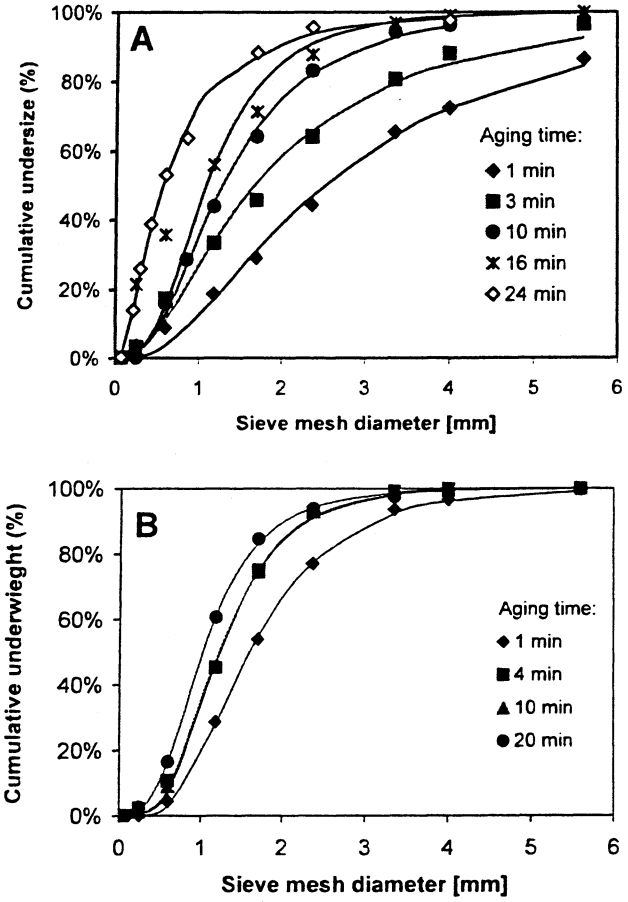

Figure 8. Cumulative underweight particle-size distributions.

At different acidification times. (A) Acidification time 1 min; (B) Acidification time 6 min. Temperature 40°C; stirring rate 500 rpm. Markers: experimental; lines: fit lognormal distribution.

but it will also increase the breakup rate. Figure 10 shows a strong decrease in particle size when increasing the stirring rate. While a stirring rate of 500 rpm, which corresponds with an average power input of 0.03 W/kg, results in mean particle sizes of 1.8–3.0 mm, a stirring rate of 750 rpm (0.1 W/kg) gives mean particle sizes of 0.2–1.4 mm. The decrease in particle size indicates that the power input has a stronger effect on the breakup of particles than on aggregation, in this regime. The fact that the mixing time is shorter at higher stirring rates may have attributed to a smaller particle size. Local overshoots in pH—where high aggregation rates can be expected—will be smaller at higher stirrer speeds. The effects of pH overshoots in casein precipitation will be explored in detail in a subsequent article.

Influence of the temperature and the amount of acid added

The influence of temperature and final pH have been extensively studied quantitatively by Jablonka and Munro (1985, 1986, 1987). Jablonka and Munro found that the particle size and calcium content increase with temperature, particularly at high pH. It was suggested that the calcium binding was a

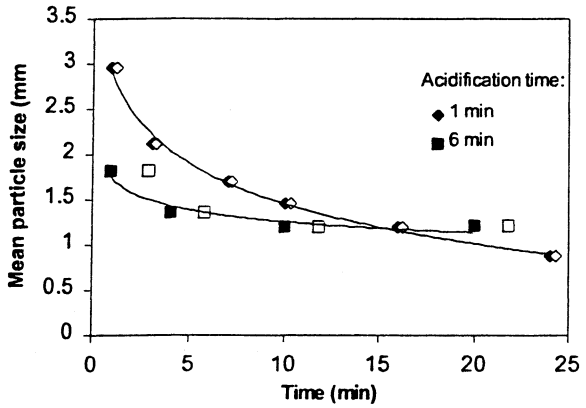

Figure 9. Influence of aging on the mean particle size at different acidification times.

For closed symbols: *x*-axis shows aging times. For open symbols, *x*-axis shows time after tcoag. Temperature: 40°C; stirring rate 500 rpm.

cause for the higher particle size (Teo et al. 1996a). The results on the influence of temperature that were found in this study (Figure 11) are qualitatively in accordance with those results in the literature. A strong increase in particle size is found when temperature is increased.

The influence of the amount of acid that was added was small in the range that was investigated. The amounts of acid that were added corresponded to pH values between 4.6 and 4.85 (Figure 12). The results are in accordance with the experiments in which the acid addition rate was changed after 85% of acid was added (Table 6). Jablonka et al. (1985) found that the final pH had a much larger influence on the particle size, possibly because they precipitated at higher acidification rates.

Solids content of the precipitate

The solids content of the precipitate increased slightly with the acidification time, regardless of whether short or long aging times were applied. The values found in this work lie in

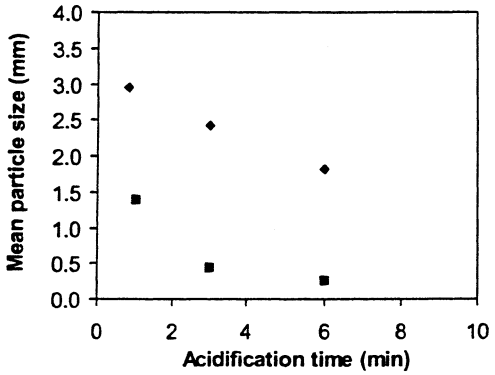

Figure 10. Influence of stirring rate on the mean particle size at different acidification times: ♦ 500 rpm; ■ 750 rpm. Temperature: 40°C; aging time 1 min.

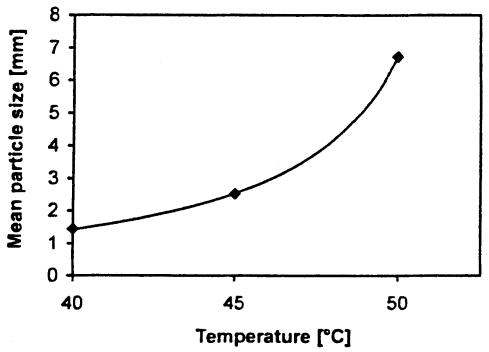

Figure 11. Influence of temperature to particle size at an acidification time of 4 min, aging period of 10 min, and a stirring rate of 500 rpm.

the same range as those found by Jablonka and Munro (1986) and Teo et al. (1996a). At an aging time of 10 min, the solids content decreased linearly from 19.9% at an acidification time of 1.5 min to 17.6% at 16 min. Aging itself had a positive effect on the measured solids content. At an acidification time of 6 min, the solids content rose from 16.9% to 21.5% when the aging period increased from 1 min to 20 min.

The decrease in the solids content with increasing acidification time is counterintuitive. The particle packing in the precipitate is expected to be less dense when the precipitation is fast, which would result in an increase in the solids content with acidification time. The observed decrease can be explained as an effect of the particle size (distribution) on the draining from the whey out of the curd. When the particle size is smaller, draining of the whey will proceed less well. More liquid will therefore be retained at longer acidification times where particle sizes are smaller.

The increase in solids content with aging time cannot be explained by this error in the experimental method, as the particle size decreases during aging. The magnitude of the increase may, however, be underestimated. The increase in solid content may be due to the rearrangement of the particles or shrinkage due to the whey being expelled from the precipitate. The results suggest that a part of the size reduction shown in Figure 9 can be attributed to the compacting of the particles.

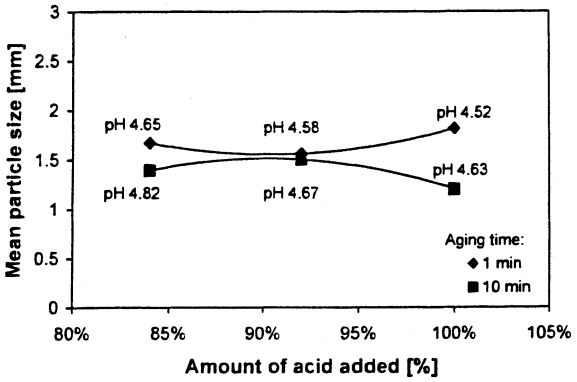

Figure 12. Influence of the amount of acid added to the reconstituted milk.

The acidification rate was kept constant at 8.33 mL/min, which corresponds with an acidification time of 6 min at standard conditions. Stirring speed 500 rpm; temperature: 40°C. Labels denote the pH at the time of measurement.

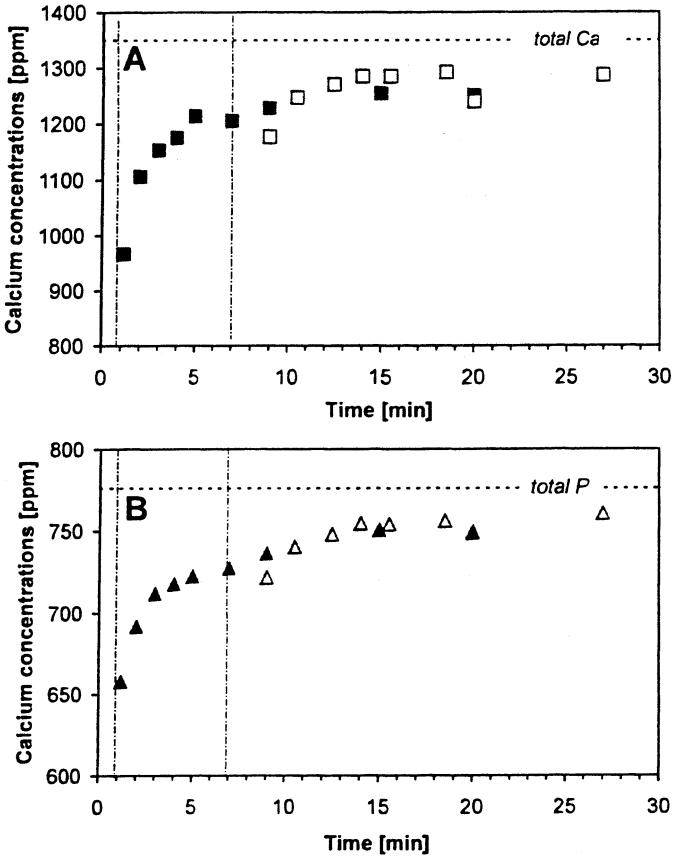

Figure 13. (A) Calcium and (B) phosphate concentrations in the whey during acidification at different acidification rates.

Closed symbols 1 min and open symbols 10 min. Lines represent calculations (see text). Vertical lines denote the times at which precipitation became visible.

Calcium phosphate release from the precipitate

The mineral concentrations in the whey were measured off-line for two experiments that differed in the acidification time (1 min and 10 min). The concentrations were measured shortly after the precipitate became visible and again at several aging times. Figure 13 shows that upon fast acidification (1 min) the whey concentrations of calcium and phosphorus-containing components rise from 965 ppm to 1,250 ppm, and 658 ppm to 749 ppm, respectively. The concentrations directly after particle formation were lower than expected on the basis of the characteristic time analysis. Le Graët and Gaucheron (1999) found that over 90% of the calcium and close to 100% percent of the inorganic phosphate are released at pH 5.1. Here only 73% of the calcium and 85% of the total phosphorus were released at 1 to 2 minutes after particle formation began. When it is assumed that diffusion out of the micelles is not an issue, it must be the dissolution

of the micellar calcium phosphate that is causing the delay. Also for the experiment with an acidification time of 10 min, the mineral concentrations start at low values, which suggest that the calcium phosphate dissolution is a slow process at and above the pH at which the particles are formed.

The acidification time does not seem to greatly influence the final release of calcium and phosphate from the precipitate. The whey phase concentrations are a little lower in the case of the short acidification time experiment.

The rate of calcium and phosphate release is also similar in both experiments, despite the difference in particle size. After a total processing time of 10 min, the whey concentrations reached similar values. The breakup of particles will be an important factor in the release rate. The breakup of the particles will bring the inner parts of any particles that still have high mineral concentrations to the surface. Particle breakup will therefore complicate the modeling of the mineral release. On the other hand, these release measurements may be useful in verifying the validity of models for particle breakup.

Conclusions

Analysis of the characteristic times showed that the most important mechanical steps in the acid precipitation of casein were acid mixing, aggregation/breakup, and transport in/out of the precipitate particles. Experimental results also indicated that besides these steps, the dissolution of the calcium phosphate also may be important for the release profiles of these process components. The particle size appeared to be strongly influenced by the dynamics of the process. Particularly, the rate of acidification was found to be important, but only for the period that the actual aggregation took place. Particle formation was found to be largely completed before the total amount of acid was added. The use of final pH as a parameter for the particle size is therefore not recommended.

Notation

D = diffusivity in liquid phase, $m^2 \cdot s^{-1}$
D_p = diffusivity in the particle, $m^2 \cdot s^{-1}$
d_m = diameter micelles, m
d_0 = diameter of the feeding tube, m
d_p = particle diameter, m
d_s = impeller diameter, m
d_t = tank diameter, m
G = mean shear rate, s^{-1}
h_t = tank height, m
k = Boltzmann constant, J/K
m = molality, mol/kg
N_s = stirring rate, s^{-1}
N_p = power number
N_q = pumping number
r_c = circulation ratio
r_p = diameter of the particle, m
r_s = diameter of the diffusing solute, m
T = temperature, K
t = characteristic time, s^{-1}
V = liquid volume, m^3

Greek letters

α = collision efficiency
ϵ = energy dissipation rate, $W \cdot kg^{-1}$
η = dynamic viscosity, $kg \cdot m^{-1} \cdot s^{-1}$
λ_K = Kolmogorov length scale, m
λ = quotient of r_p and r_s
ν = kinematic viscosity, $m^2 \cdot s^{-1}$
ϕ = volume fraction of particles
ρ_l = density of the liquid phase, $kg \cdot m^{-3}$

Literature Cited

Bell, D. J., M. Hoare, and P. Dunnill, "The Formation of Protein Precipitates and Their Centrifugal Recovery," *Adv. Biochem. Eng. Biotechnol.*, **26**, 1 (1983).

Bhaskar, G. V., O. H. Campanella, and P. A Munro, "Effect of Agitation on the Coagulation Time of Mineral Acid Casein Curd: Application of Smoluchowski's Orthokinetic Aggregation Theory," *Chem. Eng. Sci.*, 4075 (1993).

Bird, R. B., W. E. Stewart, and E. N. Lightfoot, *Transport Phenomena*, Wiley, New York (1960)

Bringe, N. A., and J. E. Kinsella, "Acidic Coagulation of Casein Micelles: Mechanisms Inferred from Spectrophotometric Studies," *J. Dairy Res.*, **57**, 365 (1990).

Bringe, N. A., and J. E. Kinsella, "Effects of Cations and Anions on the Rate of the Acidic Coagulation of Casein Micelles: the Possible Roles of Different Forces," *J. Dairy Res.*, **58**, 195 (1991).

Brown, D. L., and C. E. Glatz, "Aggregate Breakage in Protein Precipitation," *Chem. Eng. Sci.*, **42**, 1831 (1987)

Camp, T. R., and P. C. Stein, "Velocity Gradients and Internal Work in Fluid Motion," *J. Boston Soc. Civil Eng.*, **30**, 219 (1943).

Cariç, M., *Concentrated and Dried Dairy Products*, VCH, New York (1994).

Dalgleish, D. G., and A. J. R. Law, "pH-Induced Dissociation of Bovine Casein Micelles," *J. Dairy Res.*, **56**, 727 (1989).

DeKruif, C. G., "Supra-aggregates of Casein Micelles as a Prelude to Coagulation." *J. Dairy Sci.*, **81**, 3019 (1998).

Hofland, G. W., M. van Es, L. A. M. Van der Wielen, and G. J. Witkamp, "Isoelectric Precipitation of Casein Using High Pressure CO_2," *Ind. Eng. Chem. Res.*, **38**, 4919 (1999).

Holt, C., D. G. Dalgleish, and R. Jenness, "Calculation of the Ion Equilibria in Milk Diffusate and Comparison with Experiment," *Anal. Biochem.*, **113**, 154 (1981).

Jablonka, M. S., and P. A. Munro, "Particle Size Distribution and Calcium Content of Batch-Precipitated Acid Casein Curd: Effect of Precipitation Temperature and pH," *J. Dairy Res.*, **52**, 419 (1985).

Jablonka, M. S., and P. A. Munro, "Effect of Precipitation Temperature and pH on the Mechanical Strength of Batch Precipitated Acid Casein Curd," *J. Dairy Res.*, **53**, 69 (1986).

Jablonka, M. S., and P. A. Munro, "Effect of Temperature and pH on the Continuous Pilot-Scale Precipitation of Acid Casein Curd," *N. Z. J. Dairy Sci. Technol.*, **21**, 111 (1986b).

Jablonka, M. S., and P. A. Munro, "Mechanical Properties of Lactic, Mineral Acid and Rennet Casein Curds from Commercial Plants," *N. Z. J. Dairy Sci. Technol.*, **22**, 67 (1987).

Jablonka, M. S., P. A. Munro, and G. G. Duffy, "Use of Light Scattering Techniques to Study the Kinetics of Precipitation of Mineral Acid Casein from Skim Milk," *J. Dairy Res.*, **55**, 179 (1988).

Janssen, L. P. B. M., and M. M. C. G. Warmoeskerken, *Transport Phenomena Data Companion*, Edward Arnold/DUM, Delft, The Netherlands (1987).

Kim, B. Y., and J. E. Kinsella, "Effect of Temperature and pH on the Coagulation of Casein," *Milchwissenschaft*, **44**, 622 (1989).

Le Graët, Y., and F. Gaucheron, "pH-Induced Solubilization of Minerals from Casein Micelles: Influence of Casein Concentration and Ionic Strength," *J. Dairy Res.*, **66**, 215 (1999).

O'Meara, G. M., and P. A. Munro, "The Precipitation and Shrinkage of Acid Casein Curd: A Preliminary Study," *N. Z. J. Dairy Sci. Technol.*, **17**, 147 (1982).

Nelson, C. D., and C. E. Glatz, "Primary Particle Formation in Protein Precipitation," *Biotechnol. Bioeng.*, **27**, 1435 (1985).

Pearce, K. N., R. J. Johnstone, and A. J. Maccoll, "Computer Simulation of Continuous Counter-Current Washing of Casein Curd," *N. Z. J. Dairy Sci. Technol.*, **22**, 49 (1987).

Smit, D. J., M. J. Hounslow, and W. R. Paterson, "Aggregation and Gelation—I. Analytical Solutions for cst and Batch Operation," *Chem. Eng. Sci.*, **49**, 1025 (1994).

Söhnel, O., and J. Garside, *Precipitation; Basic Principles and Industrial Applications*, Butterworth-Heinemann, Oxford (1992).
Southward, C. R., and N. J. Walker, "The Manufacture and Industrial Use of Casein," *N. Z. J. Dairy Sci. Technol.*, **15**, 201 (1980).
Stryer, L., *Biochemistry*, 3rd ed., Freeman, New York (1988).
Teo, C. T., P. A. Munro, and H. Singh, "Effects of pH and Temperature on the Water-Holding Capacity of Casein Curds and Whey Protein Gels," *J. Dairy Res.*, **6**, 83 (1996a).
Teo, C. T., P. A. Munro, and H. Singh, "Reversibility of Shrinkage of Mineral Acid Casein Curd as a Function of Ionic Strength, pH and Temperature," *J. Dairy Res.*, **63**, 555 (1996b).
Thoenes, D., *Chemical Reactor Development; from Laboratory Synthesis to Industrial Production*, Kluwer, Dordrecht, The Netherlands (1994).
Van Dijk, H. J. M., "The Properties of Casein Micelles. 2. Formation and Degradation of the Micellar Calcium Phosphate," *Neth. Milk Dairy J.*, **44**, 111 (1990).
van Leeuwen, M. L. J., O. S. L. Bruinsma, and G. M. van Rosmalen, "Influence of Mixing on the Product Quality in Precipitation," *Chem. Eng. Sci.*, **51**, 2595 (1996).
Vanni, M., "Approximate Population Balance Equations for Aggregation-Breakage Process," *J. Colloid Interface Sci.*, **221**, 143 (2000).
Vonk, P., *Diffusion of Large Molecules in Porous Structures*, PhD Diss., Univ. of Groningen, Groningen, The Netherlands (1994).
Walstra, P., "On the Stability of Casein Micelles," *J. Dairy Sci.*, **73**, 1965 (1990).
Wilcox, W. R., S. Russo, and S. H. Bauer, "Cluster Size Distribution from Homogeneous Condensation. A Stochastic Model," *J. Phys. Chem.*, **83**, 897 (1979).

Manuscript received Dec. 7, 2001, and revision received Feb. 5, 2003.